SiH, SiSi, and CH Bond Activation by Coordinatively Unsaturated $RhCl(PH_3)_2$. Ab Initio Molecular Orbital Study

Nobuaki Koga and Keiji Morokuma*

Contribution from the Institute for Molecular Science, Myodaiji, Okazaki 444, Japan

Received January 4, 1993

Abstract: SiH bond activation, oxidative addition of the SiH bond of SiH_4 to coordinatively unsaturated $RhCl(PH_3)_2$, was theoretically investigated with an ab initio molecular orbital (MO) method, and its potential energy profile was compared with that for CH bond activation, oxidative addition of the CH bond of CH_4. All the stationary points were determined at the MP2 level. While CH bond activation passes through an η^2-CH_4 complex and a three-centered transition state, SiH bond activation is downhill and the η^2-SiH_4 complex is a transition state for intramolecular rearrangement connecting two silyl hydride complexes, the products of SiH bond activation. This difference originates from the much larger exothermicity of SiH bond activation due to the weaker SiH bond and the stronger RhSi bond compared with the C counterparts. The RhSi bond is about 20 kcal/mol stronger than the RhC bond; the large electron donation from SiH_3 to Rh can take place in the late transition metal complex to stabilize the electropositive silyl group. However, the order in M–R bond strength depends on the transition metal. In the Zr complex, a strong back-donation from Zr to CH_3 takes place because of the small electronegativity of Zr, resulting in the ZrC bond being stronger than the ZrSi bond. For Si_2H_6, activation of both the SiH and the SiSi bond takes place easily, and $RhCl(PH_3)_2(SiH_3)_2$ and $HRhCl(PH_3)_2(Si_2H_5)$ can rearrange with each other intramolecularly. Also, the electron correlation effect on structure and energetics is discussed.

I. Introduction

Oxidative addition of the hydrosilane SiH bond is one of the essential steps in the widely accepted mechanism of hydrosilation catalyzed by late transition metal complexes.[1] Because of the importance of hydrosilation in synthesizing organosilicon compounds and, in general, organic synthesis, SiH bond activation and interaction between the central metal and this bond has recently drawn substantial attention.[2-5]

Analogous CH bond activation, activation of an inert CH bond of a hydrocarbon,[6] was developed in the 1980s, starting with the experimental findings by Graham,[7] Bergman,[8] and Jones[9] and their co-workers. Experimental, mechanistic studies of this CH bond activation have shown that CH bond activation is achieved by CH bond oxidative addition to coordinatively unsaturated transition metal complex intermediates.[6]

Under these circumstances, theoretical analysis of these important bond activations and comparison between them would give some new insights. As to CH bond activation, several reactions have been studied with the ab initio molecular orbital (MO) method,[10-15] the extended Hückel method,[16] and density functional theory.[17] In these studies, CH bond activation by coordinatively unsaturated complexes has been found to have low activation energies. Sakaki et al. have compared reaction of CH_4 and SiH_4 with $Pt(PR_3)_2$ with the ab initio MO method to show that SiH bond oxidative addition is easier with the lower activation barrier and the larger exothermicity.[18]

In the present paper, we will report the results of ab initio MO calculations of CH and SiH bond activation by a model coordinatively unsaturated Rh complex, $RhCl(PH_3)_2$, **1**, for CH_4 and SiH_4 (eqs 1 and 2). Reaction 1 is a model of CH activation

$$\underset{\mathbf{1}}{CH_4} + \underset{\mathbf{1}}{RhCl(PH_3)_2} \rightarrow \underset{\mathbf{2}}{HRhCl(PH_3)_2(CH_3)} \quad (1)$$

$$\underset{\mathbf{1}}{SiH_4} + \underset{\mathbf{1}}{RhCl(PH_3)_2} \rightarrow \underset{\mathbf{3}}{HRhCl(PH_3)_2(SiH_3)} \quad (2)$$

(1) (a) Ojima, I. In *The Chemistry of Organic Silicon Compounds*; Patai, S., Rappoport, Z., Eds.; Wiley: New York, 1989; Part 2, p 1480. (b) Don Tilley, T. in ref. 1a, p 1415. (c) Seitz, F.; Wrighton, M. S. *Angew. Chem., Int. Ed. Engl.* **1988**, *27*, 289.

(2) (a) Lichtenberger, D. L.; Rai-Chaudhuri, A. *J. Am. Chem. Soc.* **1989**, *111*, 3583. (b) Lichtenberger, D. L.; Rai-Chaudhuri, A. *J. Am. Chem. Soc.* **1990**, *112*, 2492.

(3) Schubert, U. *Adv. Organomet. Chem.* **1990**, *30*, 151.

(4) Hester, D. M.; Sun, J.; Harper, A. W.; Yang, G. K. *J. Am. Chem. Soc.* **1992**, *114*, 5234.

(5) Rabaa, H.; Saillard, J.-Y.; Schubert, U. *J. Organomet. Chem.* **1987**, *330*, 397.

(6) For reviews of CH bond activation, see: (a) Shilov, A. E. *Activation of Saturated Hydrocarbons by Transition Metal Complexes*; D. Reidel Publishing: Dordrecht, 1984. (b) Bergman, R. G. *Science* **1984**, *223*, 902. (c) Crabtree, R. H. *Chem. Rev.* **1985**, *85*, 245. (d) Green, M. L. H.; O'Hare, D. *Pure Appl. Chem.* **1985**, *57*, 1897. (e) Jones, W. D.; Feher, F. J. *Acc. Chem. Res.* **1989**, *22*, 91.

(7) (a) Hoyano, J. K.; Graham, W. A. G. *J. Am. Chem. Soc.* **1982**, *104*, 3723. (b) Hoyano, J. K.; McMaster, A. D.; Graham, W. A. G. *J. Am. Chem. Soc.* **1983**, *105*, 7190.

(8) (a) Janowicz, A. H.; Bergman, R. G. *J. Am. Chem. Soc.* **1982**, *104*, 352. (b) Janowicz, A. H.; Bergman, R. G. *J. Am. Chem. Soc.* **1983**, *105*, 3929. (c) Periana, R. A.; Bergman, R. G. *Organometallics* **1984**, *3*, 508. (d) Wax, M. J.; Stryker, J. M.; Buchanan, J. W.; Kovac, C. A.; Bergman, R. G. *J. Am. Chem. Soc.* **1984**, *106*, 1211. (e) Janoxicz, A. H.; Periana, R. A.; Buchanan, J. W.; Kovac, C. A.; Stryker, J. M.; Wax, M. J.; Bergman, R. G. *Pure Appl. Chem.* **1984**, *56*, 13. (f) Periana, R. A.; Bergman, R. G. *J. Am. Chem. Soc.* **1984**, *106*, 7272.

(9) (a) Jones, W. D.; Feher, F. J. *J. Am. Chem. Soc.* **1982**, *104*, 4240. (b) Jones, W. D.; Feher, F. J. *Organometallics* **1983**, *2*, 562. (c) Jones, W. D.; Feher, F. J. *Organometallics* **1983**, *2*, 686. (d) Jones, W. D.; Feher, F. J. *J. Am. Chem. Soc.* **1984**, *106*, 1650. (e) Jones, W. D.; Feher, F. J. *Inorg. Chem.* **1984**, *23*, 2376. (f) Jones, W. D.; Feher, F. J. *J. Am. Chem. Soc.* **1985**, *107*, 620.

(10) Obara, S.; Kitaura, K.; Morokuma, K. *J. Am. Chem. Soc.* **1984**, *106*, 7482.

(11) Blomberg, M. R. A.; Brandemark, U.; Siegbahn, P. E. M. *J. Am. Chem. Soc.* **1983**, *105*, 5557.

(12) (a) Low, J. J.; Goddard, W. A. *Organometallics* **1986**, *5*, 609. (b) Low, J. J.; Goddard, W. A. *J. Am. Chem. Soc.* **1986**, *108*, 6115.

(13) Koga, N.; Morokuma, K. *J. Phys. Chem.* **1990**, *94*, 5454.

(14) (a) Blomberg, M. R. A.; Siegbahn, P. E. M.; Nagashima, U.; Wennerberg, J. *J. Am. Chem. Soc.* **1991**, *113*, 424. (b) Blomberg, M. R. A.; Siegbahn, P. E. M.; Svensson, M. *J. Phys. Chem.* **1991**, *95*, 4313. (c) Blomberg, M. R. A.; Siegbahn, P. E. M.; Svensson, M. *J. Am. Chem. Soc.* **1992**, *114*, 6095.

(15) Song, J.; Hall, M. B., submitted for publication.

(16) Saillard, J.-Y.; Hoffmann, R. *J. Am. Chem. Soc.* **1984**, *106*, 2206.

(17) Ziegler, T.; Tschinke, C.; Fan, L.; Becke, A. D. *J. Am. Chem. Soc.* **1989**, *111*, 9177.

(18) (a) Sakaki, S.; Ieki, M. *J. Am. Chem. Soc.* **1991**, *113*, 5063. (b) Sakaki, S.; Ieki, M. *J. Am. Chem. Soc.* **1993**, *115*, 2373.

0002-7863/93/1515-6883$04.00/0

Scheme I

(a) d orbitals of $RhCl(PH_3)_2$

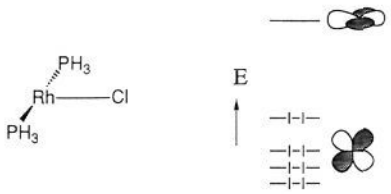

(b) Interaction between Rh d and CH σ orbitals

CH_4 Complex

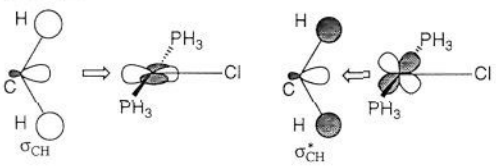

Transition State

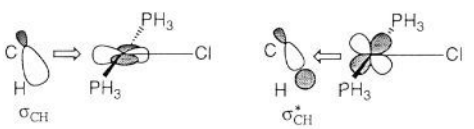

in catalytic carbonylation,[19] and we have theoretically studied this reaction in a previous paper.[13] Triethylhydrosilane has experimentally been found to add oxidatively to $RhCl(PMe_3)_2$ to afford hydrosilyl complex $HRhCl(PMe_3)_2(SiEt_3)$.[20] $HRhCl(PR_3)_2(SiR_3)$ has been considered an active intermediate in hydrosilation.[21] In recent experiments, the coordinatively unsaturated Rh complex, CpRh(CO), photochemically produced from $CpRh(CO)_2$, has been reported to activate the SiH as well as the CH bond.[22]

In the previous study,[13] we have investigated with the ab initio MO method the potential energy surface of CH bond activation of CH_4 by coordinatively unsaturated $RhCl(PH_3)_2$ (reaction 1). We have found that this model reaction actually has a low activation energy. As shown in Scheme I, coordinatively unsaturated complexes have low-lying vacant d orbitals, to which CH σ bonds of an alkane can donate electrons. This electron donation accompanied by back-donation from occupied d orbitals to CH σ^* orbitals achieves CH bond activation. We have investigated the correlation effect along the reaction coordinate determined at the restricted Hartree–Fock (RHF) level by carrying out the Møller–Plesset (MP) perturbation calculations. As a result, the electron correlation effect has been found to stabilize the product by about 40 kcal/mol relative to the reactant, and thus the transition state is reached earlier and the activation energy is lowered. Therefore, in order to obtain a more reliable potential energy profile, we determined the structures of the stationary points at the second-order Møller–Plesset (MP2) level and furthermore used a better effective core potential (ECP) for Rh, treating explicity the outermost core electrons. We also compared the energetics for reaction 1 calculated with the different correlation methods.

The order of this paper is as follows. After the Introduction and the computational methods, we present in the third and fourth sections the results for reactions 1 and 2, respectively. The comparison between CH and SiH bond activation is made in the fifth section. In the sixth section, a comparison between SiSi and SiH bond activation of Si_2H_6 by $RhCl(PH_3)_2$ is presented. In the seventh section, the MC and MSi bond strengths are compared between late and early transition metal complexes. In the eighth section, the potential energy profiles are compared with those for reactions of $Pt(PH_3)_2$. The electron correlation energy is analyzed in the ninth section. The last, tenth section is the Concluding Remarks.

II. Methods of Calculations

We determined the structures of the stationary points at the MP2 level. The C_s symmetry restriction is adopted for all the optimizations except for the cases where a higher restriction is mentioned. This is quite a reasonable assumption for the present system where no obvious theoretical or experimental reason to cause a deviation from C_s can be seen. In addition, in order to obtain better energetics and to investigate the electron correlation effect, we carried out energy calculations on the MP2 optimized structures by the full fourth-order MP4 method and the quadratic configuration interaction (QCISD)[23] method. In QCISD calculations, we also included the contribution from triple excitation by the perturbational method (QCISD(T)). For reaction 1, we also performed single and double configuration interaction (CISD) calculations. The CISD energies were corrected by the methods proposed by Davidson (CISD(D)),[24] Davidson and Silver (CISD(DS)),[25] and Pople (CISD(P)).[26]

We adopted the following three basis sets. In all the sets, we used the Hay–Wadt effective core potential which replaces core electrons up to 3d electrons and valence basis functions [3s3p3d]/(5s5p4d).[27] In the first basis set used for geometry optimization at the MP2 level, we used [3s2p]/(8s5p)[28] for C, [4s3p1d]/(11s8p1d)[28] for Si, [3s]/(4s) for H of CH_4 and SiH_4, [3s2p]/(11s8p)[28] for P and Cl, and [1s]/(4s) for H of PH_3. In the second basis set, the basis functions for PH_3 and Cl in the first basis set are recontracted as the split valence [4s3p] for P and Cl and [2s] for H of PH_3. In the last basis set used in the higher level of calculations, we adopted the same basis functions as were used in the second basis set except that we used the [3s1p]/[5s1p] for H of CH_4 and SiH_4 and added a d polarization function on C. Although the numbering seems to be random, we denote these by set III, set II, and set IV, respectively, to be consistent with the numbering in our previous paper.

We also carried out calculations of Zr methyl and silyl complexes for comparison with the Rh complexes. The basis functions and effective core potential used in these calculations were the same as those of III for the Rh complexes.

As we will show later, the difference in energy of reaction among the reactions studied here is insensitive to the basis set used. Therefore, though we calculated the potential energy profile for reactions 1 and 2 with the basis set up to IV, we used for the other reactions only basis set III, which was used in MP2 geometry optimization, and did not carry out energy calculations at the higher level. Thus, comparison was made using the results calculated at the MP2 level with basis set II for reactions 1 and 2 and basis set III for the other reactions. For clarity, we used standard notation to specify the level of calculation and the structure used. For instance, MP2/II//MP2/III designates an MP2 energy calculation with basis set II using the structure determined at the MP2 level with basis set III. All the calculations were carried out using the GAUSSIAN90 program.[29]

III. Reaction of CH_4 with $RhCl(PH_3)_2$

In Figure 1 are shown the MP2/III optimized structures with the relative energies. The energies calculated at the various levels with the two other basis sets, II and IV, are shown in Table I and Figure 2.

(19) (a) Sakakura, T.; Tanaka, M. *Chem. Lett.* **1987**, *249*, 1113. (b) Spillett, C. T.; Ford, P. C. *J. Am. Chem. Soc.* **1989**, *111*, 1932.

(20) Sakakura, T.; Abe, F.; Tanaka, M. *Abstracts*, 37th Symposium on Organometallic Chemistry, Osaka, Japan, October 1990; Paper PB203. See also: Sakakura, T.; Abe, F.; Tanaka, M. *Chem. Lett.* **1991**, 359.

(21) (a) Nagashima, H.; Tatebe, K.; Ishibashi, T.; Sakakibara, J.; Itoh, K. *Organometallics* **1989**, *8*, 2495. (b) Nagashima, H. Private communication.

(22) Drolet, D. P.; Lees, A. *J. Am. Chem. Soc.* **1992**, *114*, 4186.

(23) Head-Gordon, M.; Pople, J. A.; Raghavachari, K. *J. Chem. Phys.* **1987**, *87*, 5968.

(24) Langhoff, S. R.; Davidson, E. R. *Int. J. Quantum Chem.* **1974**, *8*, 61.

(25) Davidson, E. R.; Silver, D. W. *Chem. Phys. Lett.* **1977**, *52*, 403.

(26) Pople, J. A.; Seeger, R.; Krishnan, R. *Int. J. Quantum Chem.* **1977**, *11*, 149.

(27) Hay, P. J.; Wadt, W. R. *J. Chem. Phys.* **1985**, *82*, 270.

(28) Huzinaga, S.; Andzelm, J.; Kłbukowski, M.; Radzio-Andzelm, E.; Sakai, Y.; Tatewaki, H. *Gaussian Basis Sets for Molecular Calculations*; Elsevier: Amsterdam, 1984.

(29) Frisch, M. J.; Head-Gordon, M.; Trucks, G. W.; Foresman, J. B.; Schlegel, H. B.; Raghavachari, K.; Robb, M.; Binkley, J. S.; Gonzalez, C.; DeFrees, D. J.; Fox, D. J.; Whiteside, R. A.; Seeger, R.; Melius, C. F.; Baker, J.; Martin, R. L.; Kahn, L. R.; Stewart, J. J. P.; Topiol, S.; Pople, J. A. GAUSSIAN90; Gaussian Inc.: Pittsburgh, PA, 1990.

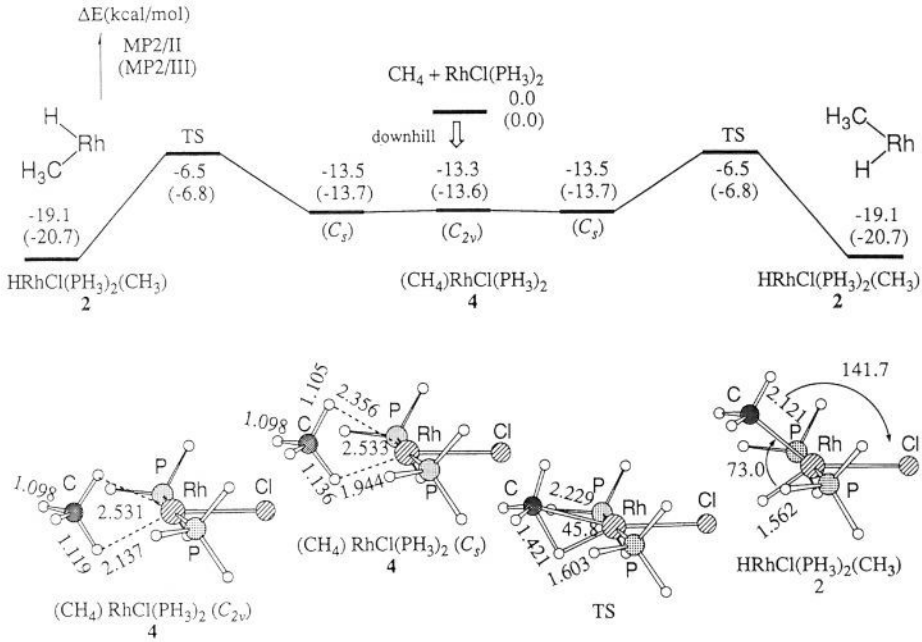

Figure 1. MP2/III optimized structures (in Å and deg) of $(CH_4)RhCl(PH_3)_2$, **4**, $HRhCl(PH_3)_2(CH_3)$, **2**, and the transition state between **4** and **2** and the MP2/II potential energy profile (in kcal/mol) for reaction of CH_4 with $RhCl(PH_3)_2$ calculated at the MP2/III optimized structures. Numbers in parentheses are at the MP2/III level. The total energy of the reactants is −1293.2577 hartrees at the MP2/III level and −1293.2974 hartrees at the MP2/II level.

Table I. Energies (in kcal/mol) with Basis Set IV for the Process $CH_4 + RhCl(PH_3)_2 \rightarrow HRhCl(PH_3)_2(CH_3)$ Relative to the Reactants for the MP2/III Optimized Structures

method	reactants[a]	CH_4 complex[b]	transition state	product
RHF	−1292.9104	−0.5	23.3	27.9
MP2	−1293.3575	−14.4	−11.1	−22.6
MP3	−1293.3964	−11.1	0.1	−6.7
MP4	−1293.4436	−15.4	−12.6	−19.3
CISD	−1293.3374	−8.9	4.4	1.5
CISD(D)	−1293.4051	−10.9	−0.6	−5.6
CISD(DS)	−1293.4365	−12.3	−4.4	−11.0
CISD(P)	−1293.4292	−12.0	−3.6	−9.9
QCISD	−1293.4438	−10.7	−2.1	−5.5
QCISD(T)	−1293.4546	−12.8	−5.1	−10.0

[a] In hartrees. [b] C_{2v} symmetric structure.

A. CH_4 Complex. For the CH_4 complex, $(CH_4)RhCl(PH_3)_2$, **4**, we determined its structure under the C_s and C_{2v} symmetry constraints. The choice of these constraints is based on the MP2//RHF calculations in our previous study where the η^2 form has been found to be the most stable.[13] In both structures, the two CH bonds interact with the Rh atom. In the symmetric C_{2v} structure, the lengths of the two interacting CH bonds are 1.119 Å, 0.02 Å longer than the noninteracting CH bonds. In the C_s structure, one CH bond interacts more strongly than the second CH bond. The CH bond with the Rh–H distance of 1.944 Å interacts more dominantly with Rh and is stretched to 1.136 Å, 0.04 Å longer than the noninteracting CH bond. The weakly interacting CH bond with the Rh–H distance of 2.356 Å is stretched to 1.105 Å, only 0.01 Å longer than the noninteracting CH bonds. The Rh–C distance is almost the same between the C_s and C_{2v} structures. Therefore, the rotation around the axis perpendicular to the mirror (paper) plane and passing through the carbon atom represents the reaction coordinate connecting the C_{2v} and C_s structures. The C_{2v} structure is not an equilibrium structure but the transition state between the two C_s structures, as shown in Figure 1. The activation barrier, the energy difference between the C_{2v} and C_s structures, is only 0.1 kcal/mol, indicating that the potential energy surface with respect to the rotation mentioned above is very flat.

The binding energy of CH_4 calculated at the MP2/III//MP2/III level is 13.6 and 13.7 kcal/mol for the C_{2v} and C_s structures, respectively. Previously, we have analyzed the origin of this binding energy in detail,[13] to show that several factors contribute to the $CH_4 \cdots RhCl(PH_3)_2$ bonding interaction; the largest contribution originates from the electron donation from the occupied σ_{CH} orbital to the Rh vacant $d_{y^2-z^2}$ orbital, supplemented significantly by the back-donation from the occupied d_{xz} orbital to the vacant σ_{CH}^* orbital, shown in Scheme I, as well as by the intermolecular correlation (dispersion) and the change in the intramolecular correlation.

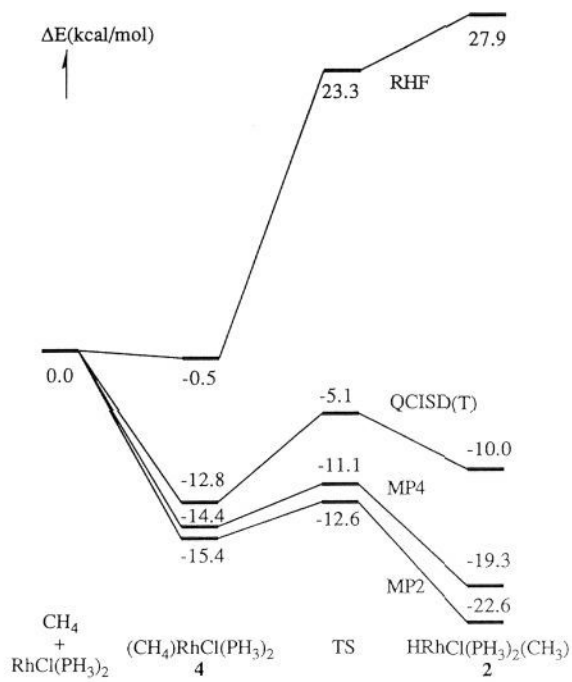

Figure 2. Potential energy profile for reaction of CH_4 with $RhCl(PH_3)_2$ calculated at various levels (in kcal/mol).

B. The Transition State for CH Bond Activation. The CH bond activation, oxidative addition of CH_4, passes through a three-centered transition state (TS). At the TS structure optimized at the MP2/III level shown in Figure 1, the distance of the CH bond to be broken is 25% longer than that of the interacting CH

bond in the C_s symmetric CH_4 complex. The RhC and RhH distances are shorter by 12% and 18%, respectively, than those in the C_s symmetric CH_4 complex and only 5% and 3% longer than those in the product. All these point to a late transition state, consistent with the exothermicity discussed later. The transition-state structure we previously found using the MP2 energy calculations along the RHF reaction path is the same within 0.07 Å in bond length as the present MP2 optimized structure. However, reflecting a large correlation effect, the structure determined here is different from the RHF transition state by as much as 0.15 Å in bond length. Because of a large *endo*thermicity at the RHF level, contrary to an *exo*thermicity at the correlated level of calculation, the RHF transition state was located artificially too late.

C. Product. Three ligands, H, CH_3, and Cl, in the mirror plane of the product take a Y-shaped structure, different from the T-shaped structure previously found at the RHF level. A comparison between the Y- and the T-shaped structure for $H_2RhCl(PH_3)_2$ at the RHF level showed that the energy difference between them was only a few kilocalories per mole. When the energy difference is small, the preference may be reversed by the electron correlation effect, and the present product is such a case. As will be shown later, qualitative features of the potential energy profile do not change whether the product is T- or Y-shaped. The correlation effect which favors the Y-shaped structure will be discussed in section IX.

D. Potential Energy Profile. In Figure 2, the potential energy profiles calculated with RHF, MP2, MP4, and QCISD(T) methods with basis set IV are shown. Those at the CISD, CISD(D), CISD(P), CISD(DS), and QCISD levels are included in Table I. One can find that the electron correlation effect is important and makes the reaction exothermic. Although the accurate absolute values of the CH_4 binding energy, the activation barrier, and the exothermicity depend strongly on the method of correlation calculation, the qualitative results do not change. CH_4 coordinates to the coordinatively unsaturated intermediate, $RhCl(PH_3)_2$, with a binding energy of more than 10 kcal/mol. The activation barrier for the oxidative addition of a CH bond relative to this CH_4 complex is small, and the TS is more stable than the dissociation limit. The isomerization between hydridomethyl complexes, or the exchange of H between hydride and methyl, can take place intramolecularly without dissociation of CH_4. The potential energy profile calculated at the MP2/IV level is similar to that at the MP2/II level. Thus, the effect of the polarization functions on C and H of CH_4 is relatively small.

For the interest of MO theoreticians, there are several comments which can be made about Table I. The MP*n* methods appear to overestimate the correlation effect compared with the other methods such as QCISD, which gives similar results with the CCSD method by Blomberg et al.[14c] Though QCISD and CCSD are believed to be more reliable, the low cost makes MP*n* calculations very useful and practical for inclusion of the correlation effect in a large transition metal complex. The MP2 energy gradient is especially cheap and is indispensable for the study of molecules with many degrees of freedom such as transition metal complexes. While the size-inconsistent CISD method underestimates the correlation effect at the transition state and the product, size-consistent corrections improve the energetics. The results corrected by the Davidson and Silver method as well as the Pople method show similar features to those obtained by the QCISD(T) method.

IV. Reaction of SiH_4 with $RhCl(PH_3)_2$

The MP2/III optimized structures of stationary points of potential surfaces are shown with their relative energies in Figure 3.

A. SiH_4 Complex. First, we determined the structure of $(SiH_4)RhCl(PH_3)_2$, **5**, under the C_{2v} symmetry constraint. In **5**, the two SiH bonds are forced to simultaneously interact with the Rh atom. The lengthening of the interacting SiH bond distance by 0.11 Å (1.605 − 1.497) in **5** is much larger than that of the CH bond distance in **4**. In addition, the Rh–H distances of 1.910 Å in **5** are shorter than those in the CH_4 complex **4**, and even the Rh–Si distance of 2.374 Å is shorter than the Rh–C distance of 2.531 Å. These results show that the Rh···SiH_4 interaction is stronger than the Rh···CH_4 interaction. The SiH_4 binding energy was calculated at the MP2/III//MP2/III level to be 25.6 kcal/mol. This is compared with 13.6 kcal/mol at the MP2/III//MP2/III level for the CH_4 complex.

The electron correlation effect enhances the SiH_4 binding to $RhCl(PH_3)_2$. The RHF/II geometry optimization gave the Rh···Si distance as 3.136 Å and the Rh–H(–Si) distance as 2.552 Å, which amount to a much longer Rh–SiH_4 distance than at the MP2 level. Consistent with this longer distance, the smaller SiH_4 binding energy of 2.1 kcal/mol was calculated at the RHF/II level. The SiH bond is softer or more polarizable than the CH bond, and thus the intermolecular correlation (dispersion) interaction is expected to be stronger in the SiH_4 complex than in the CH_4 complex. In addition, the less stable SiH σ bond orbital results in a stronger electron donation from SiH_4 to $RhCl(PH_3)_2$. According to the Mulliken population analysis, the total positive charge on SiH_4 in the complex is +0.171, which is 0.024 larger than on CH_4. These two factors strengthen the SiH_4···$RhCl(PH_3)_2$ interaction, compared with the CH_4···$RhCl(PH_3)_2$ interaction. The HSiH angle is 106.4° at the MP2/III level and 107.7° at the RHF/II level. Though the electron correlation shortens the Rh···SiH_4 distance, the nearly tetrahedral structure does not change. The tetrahedral structure also suggests that hypervalency does not play a role in this stronger SiH_4···$RhCl(PH_3)_2$ interaction.

Note in Figure 3 that, different from the CH_4 complex in Figure 1, the SiH_4 complex is not an equilibrium structure. The C_s geometry optimization, starting from the structure where one of the SiRhH angles is 5° larger than that of **5**, converged to **3**, showing that this C_{2v} SiH_4 complex is not a stable intermediate, but instead the transition state between **3** and **3'**, and that the familiar three-centered transition state for oxidative addition does not exist. Although η^1 and η^3 structures, where one and three SiH bonds, respectively, interact with Rh, may be possible, the above results indicate that in such structures one of the SiH bonds would easily break to lead to **3**.

B. Product. The optimized structure of $HRhCl(PH_3)_2(SiH_3)$, **3**, is Y-shaped with an HRhSi angle of 69.0°, though the HRhCl angle of 154.4° is larger than the SiRhCl angle of 136.6°, showing the deviation from a Y-shaped structure. The RhCl and RhH bond distances are similar to those in $HRhCl(PH_3)_2(CH_3)$, **2**.

This structure may be compared with the X-ray structure of $HRhCl(SiCl_3)(PPh_3)_2$.[30] The calculated RhSi distance of 2.325 Å is 0.12 Å longer than the experimental RhSi distance of 2.203 Å. Note that the MSi bond distances strongly depend on substituents on Si,[1b] and the halogen substituent is expected to make the RhSi bond stronger and thus shorter due to the Rhπ → Siπ back-donation. For instance, experiments[31] have shown that the CoSi distance in $(OC)_4Co(SiH_3)$ is longer than that in $(OC)_4Co(SiCl_3)$ by 0.13 Å, similar to the above difference. The experimental RhSi distance in $Cp^*Rh(SiEt_3)_2H_2$, containing no halogen substituent, is actually 2.379 Å,[32] much longer than the 2.203 Å discussed above. Theoretical calculations also support this justification; the optimized RhSi distance in $HRhCl(SiH_2F)(PH_3)_2$, 2.290 Å, is slightly shorter than the 2.325 Å above without an F substituent.

Note that at the RHF/II level, **3** does not exist. The geometry optimization at the RHF/II level converged to a sort of SiH_4

(30) (a) Muir, K. W.; Ibers, J. A. *Inorg. Chem.* **1970**, *9*, 440. (b) Manojlovic-Muir, L.; Muir, K. W.; Ibers, J. A. *Inorg. Chem.* **1970**, *9*, 447.
(31) (a) Robinson, W. T.; Ibers, J. A. *Inorg. Chem.* **1967**, *6*, 1208. (b) Robiette, A. G.; Sheldrick, G. M.; Simpson, R. N. F.; Aylett, B. J.; Campbell, J. A. *J. Organomet. Chem.* **1968**, *14*, 279.
(32) Fernandez, M.-J.; Bailey, P. M.; Bentz, P. O.; Ricci, J. S.; Koetzle, T. F.; Maitlis, P. M. *J. Am. Chem. Soc.* **1984**, *106*, 5458.

Table II. Energies (in kcal/mol) with Basis Set IV for the Process $SiH_4 + RhCl(PH_3)_2 \rightarrow HRhCl(PH_3)_2(SiH_3)$ Relative to the Reactants for the MP2/III Optimized Structures

method	reactants[a]	SiH_4 complex[b]	product
RHF	−1543.8659	10.6	−5.3
MP2	−1544.2617	−25.2	−58.4
MP3	−1544.3037	−13.4	−39.5
MP4[c]	−1544.3313	−27.5	−55.1
QCISD	−1544.3538	−18.1	−40.7
QCISD(T)	−1544.3634	−21.4	−44.6

[a] In hartrees. [b] Transition state for rearrangement. [c] MP4 without triple excitations.

complex with a side-on coordination of one SiH bond. The importance of the electron correlation effect is again demonstrated.

C. Potential Energy Profile. As mentioned above, the SiH_4 complex is not an equilibrium structure but a transition state. SiH_4 reacts with $RhCl(PH_3)_2$, without forming a $(SiH_4)RhCl(PH_3)_2$ intermediate complex and without a barrier, to give the SiH oxidative addition product $HRhCl(PH_3)_2(SiH_3)$. The isomerization between hydridosilyl complexes, or the exchange of H between hydride and silyl, can take place intramolecularly without dissociation of SiH_4. At the MP2/II level, the SiH_4 binding energy is 23.1 kcal/mol and the overall exothermicity of SiH bond activation is 55.2 kcal/mol. These values are quite different from those for reaction of CH_4, 13.5 and 19.1 kcal/mol, respectively. The higher order MP and QCISD calculations shown in Table II do not change this trend; the reaction of SiH_4 is 33–40 kcal/mol more exothermic, and the SiH_4 complex, the transition state for intramolecular rearrangement, is 2–12 kcal/mol more stable than the CH_4 complex. Energies relative to the reactants are slightly dependent on the computational method; the MP2 and MP4 methods overestimate the electron correlation effect, compared with the QCISD(T) calculations, while the MP3 method underestimates it. However, at the cheapest MP2 level, the qualitative feature of the potential energy profile is obtained correctly as in the reaction of CH_4.

V. Comparison between CH and SiH Bond Activation

The potential energy profile for SiH bond activation, reaction 2, in Figure 3 is quite different from that for CH bond activation, reaction 1, in Figure 1. This difference originates from the much larger exothermicity of reaction 2; reaction 2 is more exothermic by about 33–40 kcal/mol. This large exothermicity, in other words the stability of the product, shifts the energy of the structure corresponding to the three-centered transition state down. Eventually, such a structure becomes more stable than the SiH_4 complex and disappears, leaving the SiH_4 complex behind to become a transition state. Therefore, it is necessary to investigate the reason for the large exothermicity of reaction 2.

A. RhH, RhC, and RhSi Bond Energies. Formally, the energies of reactions 1 and 2 can be represented using bond dissociation energies by

$$D_e(H_3X\text{–}H) - D_e(Rh\text{–}XH_3) - D_e(Rh\text{–}H) \qquad (X = C, Si) \tag{3}$$

where Rh stands for the $RhCl(PH_3)_2$ fragment. Therefore, the difference in the energy of reaction between CH and SiH bond activation is

$$E_1 - E_2 = D_e(H_3C\text{–}H) - D_e(H_3Si\text{–}H) - [D_e(Rh\text{–}CH_3) - D_e(Rh\text{–}SiH_3)] \tag{4}$$

where E_i is the energy of reaction i. Accordingly, the difference in the energy of reaction can be interpreted in terms of the difference in bond dissociation energy. $D_e(H_3X\text{–}H)$ can be easily calculated directly as the energy difference between XH_4 and the dissociation limit, $XH_3 + H$. We have already calculated E_1 and E_2. Using these values, $D_e(Rh\text{–}CH_3) - D_e(Rh\text{–}SiH_3)$ can be obtained. An advantage of this method is that the error due to approximation in computational methods would be canceled in taking differences and that we can avoid direct calculation of $D_e(Rh\text{–}XH_3)$, which is more difficult than that of $D_e(H_3X\text{–}H)$.

At the MP2/II//MP2/III (RHF/II//MP2/III) level, $D_e(H_3C\text{–}H)$ and $D_e(H_3Si\text{–}H)$ were calculated to be 98.7 (84.6) and 83.0 (73.9) kcal/mol, respectively. The CH bond is stronger than the SiH bond by 15.7 (10.7) kcal/mol. Although these binding energies are underestimated, the trend that the CH bond is stronger than the SiH bond is well reproduced. Experimentally, the CH bond in CH_4 is 14.5 kcal/mol stronger than the SiH bond in SiH_4.[33] E_1 and E_2 as well as the CH and SiH bond energy difference give $D_e(Rh\text{–}CH_3) - D_e(Rh\text{–}SiH_3) = -20.4$ (−22.3) kcal/mol at the MP2/II//MP2/III (RHF/II/MP2/III) level. Thus, the RhSi bond is stronger than the RhC bond by about 20 kcal/mol. This result demonstrates that in reaction 2, relative to reaction 1, the weaker SiH bond (by 16 kcal/mol than the CH bond) is broken and the stronger RhSi bond (by 20 kcal/mol than the RhC bond) is formed, and it is more exothermic (by about 36 kcal/mol) than reaction 1.

We can confirm this by obtaining $D_e(Rh\text{–}CH_3)$ and $D_e(Rh\text{–}SiH_3)$ in a different way by using reactions 5 and 6. $D_e(Rh\text{–}CH_3)$ and $D_e(Rh\text{–}SiH_3)$ can be represented by $[D_e(H_3C\text{–}CH_3) - E_5)]/2$ and $[D_e(H_3Si\text{–}SiH_3) - E_6)]/2$, respectively. The structures of **7** and **6** optimized at the MP2/III level are shown in Figures 4 and 5, respectively. They are Y-shaped, similar to **3** and **2**. Energies of reaction were calculated to be −23.8 (+34) and −82.4 (−11) kcal/mol for reactions 5 and 6, respectively, at the MP2/III//MP2/III (RHF/III//MP2/III) level. Reaction 6 is more exothermic than the other, as expected because of the stronger RhSi bond formed and the weaker SiSi bond broken. At the MP2/III//MP2/III (RHF/III//MP2/III) level, $D_e(H_3Si\text{–}SiH_3)$ and $D_e(H_3C\text{–}CH_3)$ were calculated to be 73.1 (56.9) and 85.3 (62.9) kcal/mol, respectively. Thus, we obtain $D_e(Rh\text{–}SiH_3)$ = 77.8 (33.9) kcal/mol and $D_e(Rh\text{–}CH_3)$ = 54.6 (14.6) kcal/mol at the MP2/III//MP2/III (RHF/III//MP2/III) level; the RhSi bond is 23.2 (19.3) kcal/mol stronger than the RhC bond, the same conclusion as the above mentioned results within the error due to the approximation in the present calculations. Note that the correlation effect on the difference in bond strength and thus in energy of reaction is small; at the RHF/II//MP2/III level, reaction 2 is more exothermic than reaction 1 by 33.0 kcal/mol, which is similar to 36.1 kcal/mol at the MP2/II//MP2/III level. The $D_e(Rh\text{–}CH_3)$ obtained above and the energy of reaction 1 give $D_e(Rh\text{–}H)$ as 65.1 kcal/mol at the MP2/III level. The corresponding $D_e(Rh\text{–}H)$ calculated from $D_e(Rh\text{–}SiH_3)$ and the energy of reaction 2 is 64.8 kcal/mol. Consequently the order of bond strength at the MP2/III level is Rh–Si > Rh–H > Rh–C with about 10 kcal/mol difference between each neighbor.

$$C_2H_6 + RhCl(PH_3)_2 \rightarrow \underset{\mathbf{6}}{RhCl(PH_3)_2(CH_3)_2} \tag{5}$$

$$Si_2H_6 + RhCl(PH_3)_2 \rightarrow \underset{\mathbf{7}}{RhCl(PH_3)_2(SiH_3)_2} \tag{6}$$

Reflecting its larger bond energy, the RhSi bond is shorter than what is expected. The $H_3C\text{–}CH_3$ and $H_3Si\text{–}SiH_3$ bond distances of 1.557 and 2.363 Å at the MP2/III level suggest that the RhSi bond could be 0.403 (=(2.363 − 1.557)/2) Å longer than the RhC bond. However, the calculated RhSi bond is only 0.204 Å longer than the calculated RhC bond.

A similar result that the M–SiH_3 bond is stronger than the M–CH_3 bond has been obtained in a theoretical study of SiH_4 oxidative addition to $Pt(PH_3)_2$ by Sakaki et al.[18] Also, we have found that in the bare metal ion complex $CoXH_3^+$ (X = C, Si) the CoSi single bond is stronger than the CoC bond at the multireference CI level,[34] though the difference in bond strength

(33) *CRC Handbook of Chemistry and Physics*, 68th ed.; Weast, R. C., Ed.; CRC Press: Boca Raton, FL, 1987.

(34) Musaev, D. G.; Koga, N.; Morokuma, K., submitted for publication.

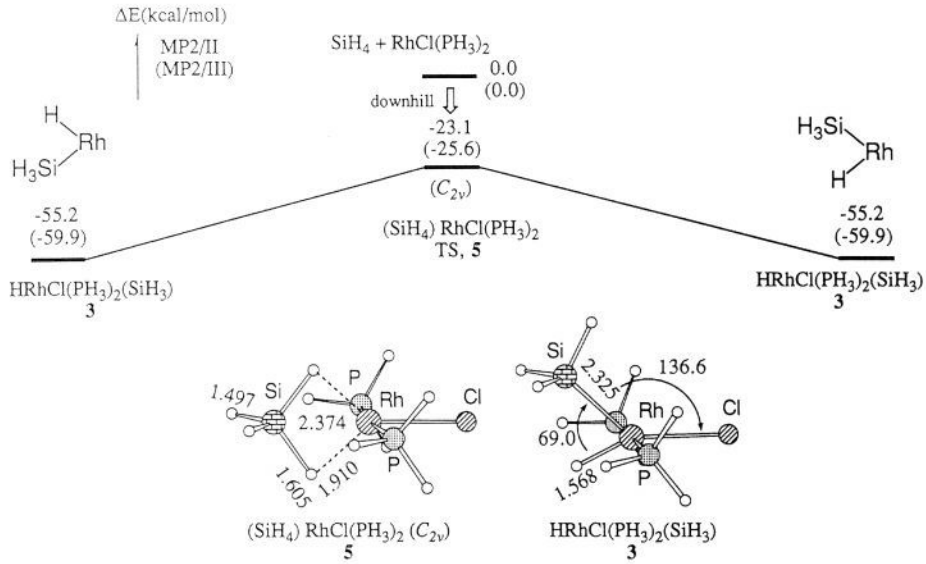

Figure 3. MP2/III optimized structures (in Å and deg) of $(SiH_4)RhCl(PH_3)_2$, **5**, and $HRhCl(PH_3)_2(SiH_3)$, **3**, and the MP2/II potential energy profile (in kcal/mol) for reaction of SiH_4 with $RhCl(PH_3)_2$ calculated at the MP2/III level. Numbers in parentheses are at the MP2/III level. The total energy of the reactants is −1544.1881 hartrees at the MP2/III level and −1544.2258 hartrees at the MP2/II level.

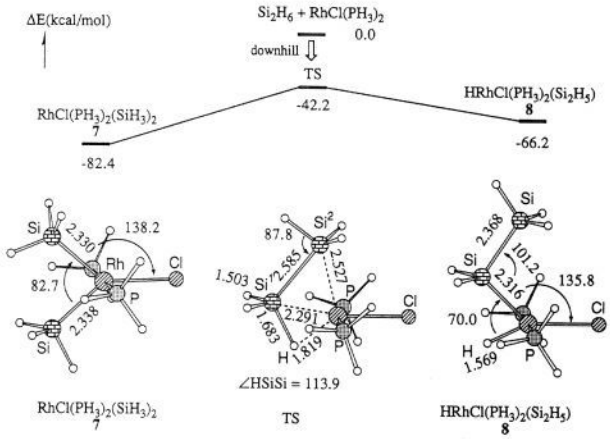

Figure 4. MP2/III optimized structures (in Å and deg) of $RhCl(PH_3)_2(SiH_3)_2$, **7**, $HRhCl(PH_3)_2(Si_2H_5)$, **8**, and the transition state between them and the potential energy profile (in kcal/mol) for reaction of Si_2H_6 with $RhCl(PH_3)_2$ calculated at the MP2/III level. The total energy of the reactants is −1834.2806 hartrees at the MP2/III level.

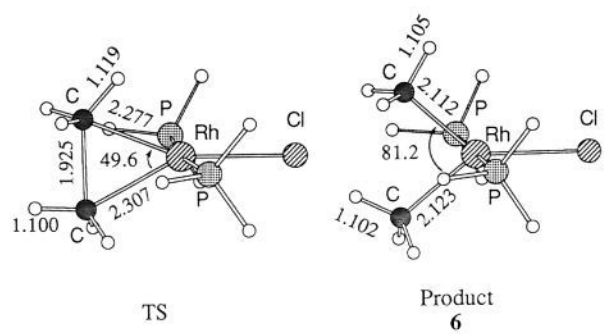

Figure 5. MP2/III optimized structures (in Å and deg) of the transition state for CC bond oxidative addition of C_2H_6 to $RhCl(PH_3)_2$ and $RhCl(PH_3)_2(CH_3)_2$, **6**. The total energy of $C_2H_6 + RhCl(PH_3)_2$ is −1332.3230 hartrees at the MP2/III level.

of 1.6 kcal/mol is small. The Mulliken charges on Co and SiH_3 in $Co(SiH_3)^+$ are +0.70 and +0.30, respectively, whereas those on Co and CH_3 in $Co(CH_3)^+$ are +0.98 and +0.02, respectively, indicating that a large electron transfer takes place from Si to Co also in this complex. The smaller energy difference in $CoXH_3^+$, compared with that in $HRhCl(PH_3)_2(XH_3)$, may be ascribed to the electrostatic repulsion between the positive charges on SiH_3 and Co. The same repulsion may be responsible for the larger difference in bond length of 0.518 Å = R(CoSi) [=2.687 Å] − R(CoC) [=2.169 Å] than 0.204 Å in $HRhCl(PH_3)_2(XH_3)$.

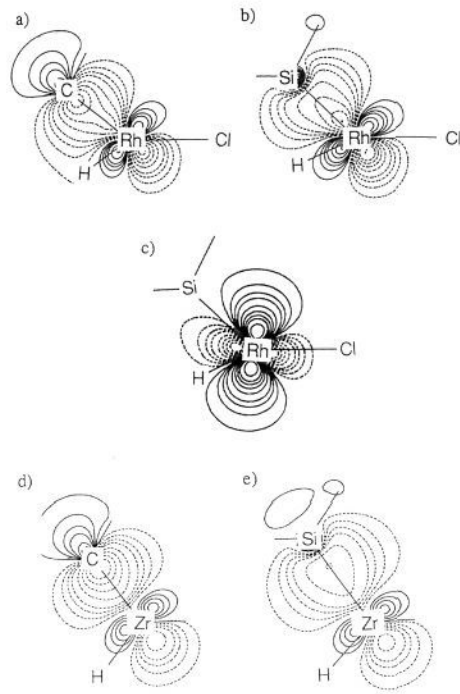

Figure 6. Boys localized molecular orbitals for (a) the RhC bond of $HRhCl(PH_3)_2(CH_3)$, **2**, (b) the RhSi bond and (c) in-plane lone pair d orbitals of $HRhCl(PH_3)_2(SiH_3)$, **3**, (d) the ZrC bond of $Cl_2Zr(CH_3)(H)$, and (e) the ZrSi bond of $Cl_2Zr(SiH_3)(H)$. The contours are ±0.3, ±0.25, ±0.2, ±0.15, ±0.1, ±0.075, ±0.05, and ±0.025 au, and solid and dotted lines denote positive and negative values, respectively.

B. Boys Localized MOs for RhC and RhSi Bonds. While an SiH bond is well-known to be weaker than a CH bond, it is not quite well established that an MSi bond is stronger than an MC bond. Therefore, we have analyzed the origin of the stronger RhSi bond. First, we calculated the Boys localized MOs (LMOs) in order to make a qualitative comparison between the RhSi and the RhC bond, as shown in Figure 6. The RhC bond seems to be more covalent with an overall Mulliken charge of −0.054 on the CH_3 group, and the RhSi bond is more ionic with a positive SiH_3 group. The electron donation from SiH_3 to Rh takes place

Scheme II

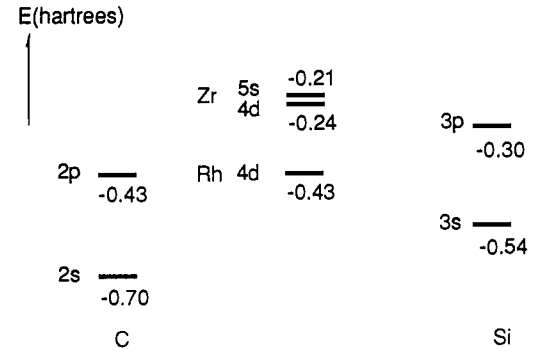

as shown by the Mulliken charge of +0.221 on the SiH_3 group. Also, there is a difference in the valence orbital between the CH_3 and the SiH_3 ligand. The orbital responsible for the Rh–CH_3 bond is the C p orbital, whereas that for the Rh–SiH_3 bond is the Si sp^3 hybrid orbital.

These differences in the bond character are understandable if one sees the atomic orbital energies. The atomic orbital energies calculated at the HF level are shown in Scheme II. The Rh d orbitals are close in energy to the C 2p orbitals, whereas they are between the Si 2s and 2p orbitals. These relationships are reflected in the order of electronegativity: C (2.5) > Rh (2.2) > Si (1.8).[35] As a result, both Si 3s and 3p orbitals interact with the Rh d orbitals to form an sp^3 hybrid orbital and to donate electrons to Rh. On the other hand, the C 2p orbitals interact with the Rh d orbitals more than the C 2s orbital, and they form a covalent RhC bond because of the similar orbital energies between the Rh d and C 2p orbitals.

C. Analysis of CH and SiH Bond Energy. Although there are clear qualitative differences between the RhC and the RhSi bond, still unresolved is the quantitative reason that the RhSi bond is so strong. Therefore, we carried out the energy decomposition analysis (EDA)[36] of the RhC and the RhSi bond energy with basis set III, in order to obtain more quantitative evidence. The EDA is carried out for the RHF bond energy. Though the electron correlation effects are definitely important in calculating energetics of the reactions, they are not essential when the bond energy of these two bonds is compared as discussed above.

In this analysis, the bond energy relative to the frozen dissociation limit, XH_3 + $HRhCl(PH_3)_2$, with each fragment having the same structure as in $HRhCl(PH_3)_2(XH_3)$, will be discussed. Thus, the bond energy, D_e(Rh–XH_3), is divided into the terms due to the exchange interaction (EX), the electrostatic interaction (ES), and the charge transfer coupled with the polarization interaction (CTPLX) from the ligand and from the metal. EX is the exchange repulsion, often called four-electron repulsion, between two fragments. ESX is the sum of EX and ES. CTPLX(Rh→XH_3) and CTPLX(Rh←XH_3) represent the interaction energy due to electron, principally odd electron, donation from the Rh fragment to the XH_3 fragment and vice versa, respectively. During the bond formation process, these two donations take place simultaneously, but in the present analysis they are analyzed separately. The negative (positive) value of each term means that it is attractive (repulsive). The calculations of the fragments were performed with the restricted open-shell (RO) HF method.[37]

The EDA results are shown in Table III. As expected, the binding energy calculated at the RHF/III level by using the frozen fragment structures shows that the RhSi bond is 15.6 kcal/mol stronger than the RhC bond. EX, an indicator of interfragment separation, is more positive for SiH_3 than for CH_3, consistent with the short Rh–Si distance discussed above. ES for SiH_3 is more negative because of the short distance and the positive charge on Si. Overall, ESX disfavors the RhSi bond more than the RhC bond. On the other hand, while CTPLX(Rh→SiH_3) is comparable to CTPLX(Rh→CH_3), CTPLX(Rh←XH_3) is much more negative for X = Si than for X = C. The results in Table III suggest that CTPLX(Rh←SiH_3) and ES are responsible for the stronger RhSi bond. However, when the interfragment separation is shorter as in $HRhCl(PH_3)_2(SiH_3)$, each interaction energy component often has a larger absolute value. In such a case, comparison of the interaction energy components at the same interfragment separation would be more desirable.

The standard protocol for this situation is to use EX as an indicator of the interfragment separation.[38] As shown in Table III, EX for $HRhCl(PH_3)_2(SiH_3)$ at the Rh–Si distance of 2.445 Å with the other structural parameters fixed to those in the optimized structure is the same as that for the optimized $HRhCl(PH_3)_2(CH_3)$ structure. CTPLX(Rh←SiH_3) of −37.9 kcal/mol is still 16 kcal/mol more negative than CTPLX(Rh←CH_3), despite the longer RhSi bond, whereas CTPLX(Rh→SiH_3) of −21.3 kcal/mol is similar to CTPLX(Rh→CH_3), and ES of −67.1 kcal/mol is now only 6 kcal/mol more negative than that for CH_3. Therefore, it is concluded that the donative interaction CTPLX(RH←SiH_3) is the most important factor of the strong RhSi bond; electron donation takes place from SiH_3 to $HRhCl(PH_3)_2$, to stabilize the system. This conclusion derived from the energetic consideration based on EDA confirms the suggestion made by the qualitative LMO discussion above.

The shorter MSi distance has been often rationalized in terms of back-donation from a metal-occupied $d\pi$ orbital to an Si $d\pi$ orbital. However, in $HRhCl(PH_3)_2(SiH_3)$ such an effect is small, as shown in the lone pair d LMO shown in Figure 6, where the contribution of the Si d orbital is quite small. EDA also shows that this back-donation CTPLX(Rh→SiH_3) is not responsible for the stronger RhSi bond.

As was discussed in section IVB, an electron-withdrawing group such as halogen on the Si atom shortens the RhSi bond. This is opposite to the expectation that an electron-withdrawing group would suppress CTPLX(Rh←Si) to weaken the RhSi bond. In order to investigate the origin of this discrepancy, we have carried out EDA for the interaction of SiH_2F with $HRhCl(PH_3)_2$, as shown in Table III. At the equi-EX separation, ES and CTPLX(Rh←Si) are nearly equal to those for SiH_3; the more dominant CTPLX(Rh←Si) is unchanged upon substitution. On the other hand, CTPLX(Rh→SiH2F) is 4 kcal/mol more attractive than CTPLX(Rh→SiH_3); electron back-donation from Rh to the silyl group is enhanced upon fluoro substitution, to strengthen the Rh–SiH_2F bond.

VI. Reaction of Si_2H_6 with $RhCl(PH_3)_2$

A large affinity of Si with the Rh complex has stimulated us to study the reaction of Si_2H_6 with $RhCl(PH_3)_2$; the activation of a CC bond is usually harder than that of a CH bond, and we would like to know whether a similar situation applies for SiSi vs SiH activation. In this reaction, there are two reaction paths, SiSi and SiH bond activations.

$$Si_2H_6 + RhCl(PH_3)_2 \rightarrow \underset{\mathbf{7}}{RhCl(PH_3)_2(SiH_3)_2} \quad (6)$$

$$Si_2H_6 + RhCl(PH_3)_2 \rightarrow \underset{\mathbf{8}}{HRhCl(PH_3)_2(Si_2H_5)} \quad (7)$$

A. Products. We have already shown in Section VA that reaction of Si_2H_6 giving $RhCl(PH_3)_2(SiH_3)_2$, **7**, the SiSi bond

(35) Pauling, L. *The Chemical Bond*; Cornell University Press: Ithaca, 1967.

(36) (a) Kitaura, K.; Morokuma, K. *Int. J. Quantum Chem.* **1976**, *10*, 325. (b) Kitaura, K.; Sakaki, S.; Morokuma, K. *Inorg. Chem.* **1981**, *20*, 2292.

(37) The EDA calculations were performed with the IMSPACK program: Morokuma, K.; Kato, S.; Kitaura, K.; Ohmine, I.; Sakai, S.; Obara, S. IMS computer center library, No. 0372.

(38) (a) Sakaki, S.; Kitaura, K.; Morokuma, K. *Inorg. Chem.* **1982**, *21*, 760. (b) Sakaki, S.; Kitaura, K.; Morokuma, K.; Ohkubo, K. *Inorg. Chem.* **1983**, *22*, 104. (c) Nakamura, E.; Miyachi, Y.; Koga, N.; Morokuma, K. *J. Am. Chem. Soc.* **1992**, *114*, 6686.

Table III. RHF Energy Decomposition Analysis of Rh–CH_3, Rh–SiH_3, Rh–SiH_2F, Zr–CH_3, and Zr–SiH_3 Bond Energy (in kcal/mol)

	[Rh][a]					[Zr][b]		
	CH_3[c]	SiH_3[c]	SiH_3[d]	SiH_2F[c]	SiH_2F[e]	CH_3[c]	SiH_3[c]	SiH_3[f]
ESX	35.7	45.9	30.1	49.5	45.0	32.1	18.6	39.7
ES	−61.5	−87.2	−67.1	−93.6	−88.1	−73.5	−43.1	−65.9
EX	97.2	133.1	97.2	143.1	133.1	105.6	61.7	105.6
CTPLX([M]←XH_3)	−21.5	−49.7	−37.9	−53.5	−50.5	−19.5	−18.8	−26.7
CTPLX([M]→XH_3)	−23.5	−27.7	−21.3	−33.9	−32.1	−48.5	−23.8	−32.8
RES	−3.8	2.8	2.2	3.8	3.5	−15.5	−6.8	−5.3
INT	−13.1	−28.7	−26.9	−34.1	−34.1	−51.4	−30.8	−25.1

[a] [Rh] = $HRhCl(PH_3)_2$. [b] [Zr] = Cl_2ZrH. [c] MP2/III optimized structure. [d] At the Rh–Si distance of 2.445 Å, where EX is equal to that for CH_3. [e] At the Rh–Si distance of 2.318 Å, where EX is equal to that for SiH_3. [f] At the Zr–Si distance of 2.535 Å, where EX is equal to that for CH_3.

activation, is very exothermic by 92.4 kcal/mol at the MP2/III//MP2/III level. On the other hand, the exothermicity of SiH bond activation leading to $HRHCl(PH_3)_2(Si_2H_5)$, **8**, is 16.2 kcal/mol smaller as shown in Figure 4. The RhH bond in **8** is weaker than the RhSi bond in **7** as discussed above, and the H_3SiH_2Si–H bond broken in reaction **7** is stronger than the H_3Si–SiH_3 bond broken in reaction 6. These two effects combined result in the less stable **8**. However, **8** is still 66.2 kcal/mol more stable than the reactants.

B. Rearrangement between 7 and 8. The large stability of **7** and **8** reminds us of reaction of C_2H_4 with $CpRh(PH_3)$.[39] At the MP2 level, we have found that ethylene coordination to $CpRh(PH_3)$ and CH bond activation giving $CpRh(PH_3)(C_2H_3)(H)$ are exothermic by 71 and 47 kcal/mol, respectively, and that rearrangement between these two structures can take place intramolecularly without dissociation of C_2H_4. Similar to this situation, the transition state connecting **7** and **8**, shown in Figure 4, is lower in energy than $RhCl(PH_3)_2$ + Si_2H_6, and rearrangement between **7** and **8** takes place intramolecularly without Si_2H_6 dissociation.

At this transition state, the SiSi and one SiH bond interact with the Rh atom, similarly to the two SiH bonds interacting with the Rh atom simultaneously at the transition state between the two isomers of **3** in reaction 2 (cf. Figure 3). The interacting Si^1H and Si^1Si^2 bonds are much stretched at 1.683 and 2.587 Å, corresponding to the intermediate stage of the Si^1H bond breaking and the Si^1Si^2 bond forming. The RhH bond of 1.819 Å is longer than that in **8** by 16%, and the $RhSi^2$ bond of 2.527 Å is longer than that in **7** by 8%. These features in bond lengths are as expected for bond exchange from the $RhSi^2$ and the SiH^1 bond in **7** to the Si^1Si^2 and the RhH bond in **8**. Note that the $RhSi^1$ distance of 2.291 Å is shorter than that in the transition state between two isomers of **3** (cf. Figure 3), showing that Si_2H_6 interacts with Rh more strongly than SiH_4. Thus, the binding energy from Si_2H_6 + $RhCl(PH_3)_2$ to this transition state is larger than that from SiH_4 + $RhCl(PH_3)_2$ to its transition state.

The strong interaction of both SiSi and SiH bonds to $RhCl(PH_3)_2$ shows contrast to that of the carbon analogues. At the MP2/III level, the transition state for ethane CC bond oxidative addition shown in Figure 5 is less stable than C_2H_6 + $RhCl(PH_3)_2$ by +18.7 kcal/mol. This should be compared with −42.2 kcal/mol for the transition state between **7** and **8**.

VII. Comparison between Late and Early Transition Metal Complexes

In the preceding section, we have shown that electron donation from SiH_3 to Rh is the origin of the strong RhSi bond. If the electron donation from the SiH_3 ligand to a transition metal is weaker because of a smaller electronegativity of the metal, it would be expected that the corresponding metal–Si bond would be weaker in strength than the RhSi bond. For instance, in an early transition metal complex, donation from SiH_3 to high-lying d orbitals of M, CTPLX(M←SiH_3), would be difficult to take place. In order to confirm this postulate by theoretical evidence,

(39) Koga, N.; Maseras, F.; Morokuma, K. *Abstracts*, 37th Symposium on Organometallic Chemistry, Osaka, Japan, October 1990; Paper A104.

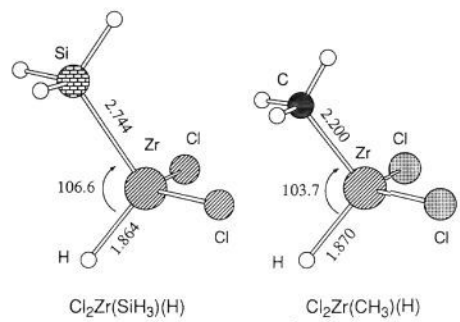

$Cl_2Zr(SiH_3)(H)$ $Cl_2Zr(CH_3)(H)$

Figure 7. MP2/III optimized structures (in Å and deg) of $Cl_2Zr(SiH_3)(H)$ and $Cl_2Zr(CH_3)(H)$.

we have calculated the bond energy difference between the ZrC and ZrSi bonds, considering Zr as an example of a more electropositive atom; in fact, the electronegativity of Zr of 1.4 is even smaller than that of Si.[34] We compared the bond energy for these bonds in $Cl_2Zr(XH_3)H$ by considering a hypothetical reaction:

$$Cl_2Zr(CH_3)H + SiH_4 \rightarrow Cl_2Zr(SiH_3)H + CH_4 \quad (8)$$

The MP2/III optimized structures of $Cl_2Zr(CH_3)(H)$ and $Cl_2Zr(SiH_3)H$ are shown in Figure 7. The energy of reaction, which corresponds to $D_e(H_3C–H) - D_e(H_3Si–H) + D_e(Zr–Si) - D_e(Zr–C)$, is 1.2 (−1.0) kcal/mol at the MP2/III//MP2/III (RHF/III//MP2/III) level. The previously obtained $D_e(H_3C–H)$ and $D_e(H_3Si–H)$ lead to $D_e(Zr–Si) - D_e(Zr–C) = -14.3$ (−11.7) kcal/mol at the MP2/III//MP2/III (RHF/III//MP2/III) level, showing that the ZrSi bond is in fact weaker than the ZrC bond, opposite to the trend found for the RhSi and the RhC bond.

In order to perform a more quantitative analysis of the origin of the stronger ZrC bond, we have carried out EDA for the RHF ZrC and ZrSi bond energies. The results are shown in Table III. CTPLX(Zr←SiH_3), the interaction which strengthened the RhSi bond, is now similar in magnitude to CTPLX(Zr←CH_3). In both CH_3 and SiH_3 complexes, on the other hand, the back-donative CTPLX(Zr→XH_3) is more negative than the donative CTPLX(Zr←XH_3). In fact, CTPLX(Zr→CH_3) of −48.5 kcal/mol is so negative that the Zr–CH_3 bond is stronger than the Zr–SiH_3 bond. The electronegativity of Zr is smaller than that of C and Si, and thus Zr tends to donate electrons to CH_3 and SiH_3. The Boys localized MOs for the ZrC and ZrSi bonds shown in Figure 6 show that these ZrC and ZrSi bonds are polarized like $Zr^{\delta+}$–$X^{\delta-}$. As shown in Scheme II, the Zr orbitals are higher in energy than those for C and Si, supporting the above discussions. In the Zr complex, electropositive Si has to receive electrons from Zr. This is very unfavorable, and therefore the ZrSi bond is weak. The relative bond strength thus strongly depends on the electronegativity of the central transition metal and the ligand.

VIII. Comparison with Reaction of $Pt(PH_3)_2$

It has been shown in the above section that the coordinatively unsaturated reactant, $RhCl(PH_3)_2$, easily breaks CH and SiH bonds as well as an SiSi bond with a strong bonding interaction

with XH_4 and Si_2H_6. As shown in the Introduction, the low-lying vacant d orbital extends around the empty coordination site where XH_4 attacks. This fact also suggests that the vacant coordination site is electron-deficient and that, therefore, the repulsion between XH_4 and $RhCl(PH_3)_2$ is small when XH_4 attacks the vacant coordination site. This small repulsion and the electron donation from XH_4 to the vacant d orbital would lower the activation barrier at the transition state and enhance the bonding interaction in the XH_4 complexes.

We have previously found that electron donation is important at the transition state of H_2 oxidative addition to $Pt(PH_3)_2$.[10] However, in this case, since all d orbitals are doubly occupied, the electron donation takes place from σ_{HH} to s and p orbitals of the Pt atom and thus is weaker. Also, the repulsion between H_2 and $Pt(PH_3)_2$ is substantial, since all the d orbitals are occupied. Therefore, the potential energy surfaces for the reactions of $Pt(PH_3)_2$ may be different from those of $RhCl(PH_3)_2$.[40] Recent theoretical studies by Sakaki and Ieki[18b] have shown that for $Pt(PH_3)_2$ the activation barriers for CH and SiH bond oxidative addition relative to the reactant complexes at the MP4 level are 30.4 and 0.7 kcal/mol. This barrier for CH bond activation is substantially higher than that for $RhCl(PH_3)_2$, and also, the transition state for SiH bond activation exists for $Pt(PH_3)_2$, whereas for $RhCl(PH_3)_2$ the reaction is downhill. This difference in the potential energy profiles shows the high reactivity of the coordinatively unsaturated complex.

IX. Analysis of the Electron Correlation Effect

The electron correlation effect is large so as to change drastically the potential energy profiles for the reactions studied, as shown above. From theoreticians' point of view, an analysis of this effect is meaningful, and thus in this section we discuss the electron correlation effect on the potential energy profiles.

The correlation effect on CH bond activation (reaction 1) has previously been analyzed in detail.[13] When the newly formed RhH and RhC bonds are covalent with a large d character, intrabond correlation for the RhH and RhC bonds and correlation between these bond electrons and metal d electrons have been found to be important. As mentioned above, the correlation effect stabilizes the Y-shaped $HRhCl(PH_3)_2(CH_3)$, **2**, more than the T-shaped **2**. In order to clarify the origin of this differential correlation effect, we analyzed the correlation energy with the LMO-MP2 method, the MP2 method based on the localized MOs (LMOs). In this method, the MP2 correlation energy is written as a sum of LMO pair correlation energies:

$$E_{MP2} = \sum_{i \geq j}^{LMO} \epsilon_{ij} \qquad (9)$$

In carrying out the analysis, we divide electrons into seven groups, as shown in Chart I: six d electrons which remain on the metal during the reaction (denoted by d(6)), two electrons in the RhH bond, two electrons in the RhC or RhSi bond, six electrons in the three nonreacting CH or SiH bonds, four electrons in the two RhP bonds, eight electrons in three Cl lone pairs and the RhCl bond, and twelve electrons in the six PH bonds.

Chart Ia,b gives the absolute values of LMO pair correlation energies $-\epsilon_{ij}$ for the T- and Y-shaped structures. The former is the same as in Chart Ic in our previous study.[13] In the upper triangle in Chart Ib is shown the difference in correlation energy between the Y- and T-shaped structures. These differences indicate clearly that, upon going from T to Y, the correlation energies related to the RhH bond decrease slightly and those related to the RhC bonds increase. In the T-shaped structure, there is no ligand trans to the hydride, whereas the ligand trans to the methyl group is Cl. The RhH bond, therefore, is more covalent and has a larger d character than the RhC bond, and thus the correlation energy of the RhH bond is larger than that of the RhC bond. On the other hand, in the Y-shaped structure the Cl ligand is trans to neither the hydride nor the methyl group. Accordingly, the RhH and RhC bonds are similar to each other in character, and thus the RhH intrabond correlation energy of 20 mhartrees is similar to that of the RhC bond of 21 mhartrees. The RhH bond becomes less covalent going from the Y-shaped structure to the T-shaped structure, and thus its correlation energy decreases, whereas the RhC bond becomes more covalent so that its correlation energy increases. Overall, the electron correlation favors the Y-shaped structure by 15.8 mhartrees.

In reaction 2, the correlation effect is similarly important; at the RHF/II level, SiH_4 dissociates from **3** without barrier to give $RhCl(PH_3)_2(SiH_4)$ with one SiH bond interacting with the Rh atom. This SiH_4 complex is more stable than **3** by 4.6 kcal/mol at the RHF/II level but less stable by 26.2 kcal/mol at the MP2/II//RHF/II level. We carried out the same analysis as shown in Chart Ic, where the upper triangle shows the difference between the Y-shaped SiH_3 and CH_3 complexes. The results show unequivocally that the electron correlation effect related to the RhSi and RhH bonds is important in the SiH_3 complex, as in the CH_3 complex. One can notice, however, significant differences between the SiH_3 and the CH_3 complex. As discussed above, the RhSi bond is more ionic with a positive charge on the Si atom than the RhC bond. In the SiH_3 complex, electron donation from the SiH_3 group reduces the covalency of the RhH bond. These factors reduce the intrabond correlation effect of the RhSi and RhH bonds. The SiH bonds are ionic with a positive charge on the Si atom. In addition, the SiH bonding electrons are better separated from the RhSi bonding electrons, compared with the situation in **2**, because of the longer RhSi bond than the RhC bond. Therefore, the electron correlation between the RhSi and SiH bonding electrons is smaller than that between the RhC and CH bonding electrons. However, the ionic RhSi bond has a larger d character as shown in Figure 6. This results in the larger inter-LMO electron correlation between the d(6) electrons and the RhSi bond electrons than that between the d(6) electrons and the RhC bond electrons. As a result, the electron correlation related to the ionic bonds of the Si atom is smaller, whereas the electron correlation between the RhSi bond electrons and the d electrons is larger. Overall, the electron correlation energy in **3** is similar or slightly smaller than that in **2**.

X. Concluding Remarks

In this paper, we have theoretically studied and compared the potential energy profile for SiH bond as well as CH bond activation by coordinatively unsaturated $RhCl(PH_3)_2$. All the stationary points were determined at the correlated MP2 level. The reaction of CH_4 with $RhCl(PH_3)_2$ passes through the η^2-CH_4 complex and a three-centered transition state. Overall energy of reaction is exothermic by 23, 19, and 10 kcal/mol at the MP2, MP4, and QCISD(T) levels, respectively. The activation barrier relative to the η^2-CH_4 complex is only 3–8 kcal/mol, and thus the CH activation by this coordinatively unsaturated complex is quite easy.

The potential energy profile for SiH bond activation is quite different. The SiH bond activation is downhill, and the η^2-SiH_4 complex is not an intermediate but the transition state for intramolecular rearrangement between two hydridosilyl complexes, the products of SiH bond activation. This difference from the reaction of CH_4 originates from the strong RhSi bond and the weak SiH bond, which results in the much larger exothermicity of the SiH bond activation than that of the CH bond activation. The RhSi bond was calculated to be 20 kcal/mol stronger than the RhC bond and the SiH bond 16 kcal/mol weaker than the CH bond. This strong RhSi bond is not consistent with the traditional view of a weaker bond of Si seen in organic chemistry. Therefore, we analyzed the reason for this strong RhSi bond to find that, in $HRhCl(PH_3)_2(SiH_3)$, strong donation from SiH_3 to

(40) Daniel, C.; Koga, N.; Han, J.; Fu, X. Y.; Morokuma, K. *J. Am. Chem. Soc.* **1988**, *110*, 3773.

Chart I. MP2/II LMO Electron Correlation Energies $-\epsilon_{ij}$ (in mhartrees) for (a) T- and (b) Y-shaped $HRhCl(PH_3)_2(CH_3)$ and (c) $HRhCl(PH_3)_2(SiH_3)$ in the Lower Triangles, the Upper Triangles of Blocks b and c Being Changes from Blocks a and b, Respectively

(a) T-shaped $HRhCl(PH_3)_2(CH_3)$[a]: $-E_{MP2}$ = 442 mhartrees.

	d(6)	RhH(2)	RhC(2)	3×CH(6)	2×RhP(4)	Cl(8)	6×PH(12)
d(6)	44						
RhH(2)	28	22					
RhC(2)	21	7	16				
3×CH(6)	3	1	26	64			
2×RhP(4)	18	6	5	2	15		
Cl(8)	6	2	2	1	3	25	
6×PH(12)	3	1	1	1	23	2	92

(b) Y-shaped $HRhCl(PH_3)_2(CH_3)$[b]: $-E_{MP2}$ = 457 mhartrees.

	d[6]	RhH	RhC	3×CH	2×RhP	Cl	6×PH
d(6)	45 +1	−1	+4	0	+1	0	0
RhH(2)	27	21 −1	+2	0	0	0	0
RhC(2)	24	9	20 +4	+1	+1	0	0
3×CH(6)	3	2	27	65 +1	0	0	0
2×RhP(4)	19	6	6	2	15 0	0	+1
Cl(8)	6	2	2	1	3	25 0	0
6×PH(12)	3	2	2	1	24	2	96 +4

(c) $HRhCl(PH_3)_2(SiH_3)$[a]: $-E_{MP2}$ = 450 mhartrees.

	d(6)	RhH(2)	RhSi(2)	3×SiH(6)	2×RhP(4)	Cl(8)	6×PH(12)
d(6)	42 +3	−5	+12	0	+2	0	0
RhH(2)	22	18 −3	+3	+1	0	0	0
RhSi(2)	36	12	17 −3	−15	+3	+1	0
3×SiH(6)	3	3	12	59 −6	0	0	+1
2×RhP(4)	21	6	9	2	16 +1	0	+1
Cl(8)	6	2	3	1	3	26 +1	0
6×PH(12)	3	2	2	2	25	2	97 +1

[a]RHF/III optimized structures.
[b]MP2/III optimized structures.

[a] RHF/III optimized structures.[b] MP2/III optimized structures.

$RhCl(PH_3)_2$ takes place to stabilize the system. This donation is larger in the electropositive SiH_3 group than in the CH_3 group. The back-donation from Rh to Si d orbital is less important than what has been considered. Although the fluorine substituent on Si enhances the back-donation to result in the shorter RhSi bond, the back-donation is still secondary in the stabilization energy.

The bond strength is shown to be different in an early transition metal complex. In the Zr complex, for instance $Cl_2Zr(SiH_3)H$, the back-donation is weaker because of the small electronegativity of Zr, and thus the ZrSi bond is weaker than the ZrC bond.

We also studied the reaction of Si_2H_6 with $RhCl(PH_3)_2$. Since the RhSi bond is so strong, the reaction giving $RhCl(PH_3)_2(SiH_3)_2$ is very exothermic by 82 kcal/mol at the MP2 level, and this disilyl complex is 16 kcal/mol more stable than $HRhCl(PH_3)_2(Si_2H_5)$. We found the transition state for intramolecular rearrangement between these two products, where the SiH and the SiSi bond interact with the Rh atom in a similar fashion as the two SiH bonds interact with the Rh atom in the transition state between two $HRhCl(PH_3)_2(SiH_3)$ molecules.

$RhCl(PH_3)_2$ is coordinatively unsaturated with a vacant d orbital, and thus it can interact with a molecule such as CH_4 and SiH_4 without any difficulty, leading to the low activation barrier or downhill reaction. Also, the rearrangement can take place intramolecularly.

The electron correlation effect on the energetics of the reactions is quite large; it makes the reaction exothermic and lowers the activation barrier. In $HRhCl(PH_3)_2(CH_3)$, the RhC and the RhH bond are covalent with large d character, and thus the intrabond correlation and the correlation with the d electrons are substantial. In $HRhCl(PH_3)_2(SiH_3)$, the RhSi bond is more ionic with $Si^{\delta+}$ because of the strong Si→Rh donation, and thus the intrabond correlation is smaller. However, the donated electrons correlate with the d electrons, and thus the correlation effect is important to the stability of the silyl complex.

Acknowledgment. This study was supported in part by grants-in-aid from the Ministry of Education, Culture, and Science of Japan. We are also grateful to Prof. S. Sakaki for valuable discussions. Part of the calculations were carried out at the Computer Center of IMS.